

“Detector walk” in position-sensitive detectors with biased microchannel plates

A. S. Tremsin,^{a)} J. V. Vallerga, and O. H. W. Siegmund

Experimental Astrophysics Group, Space Sciences Laboratory, UC Berkeley, Berkeley, California 94720

(Received 7 March 2000; accepted for publication 28 July 2000)

The spatial resolution of high-accuracy microchannel plate (MCP) detectors has reached the values, where the so-called detector walk (or image blurring) may start to limit any further improvements. Image blurring with gain is studied in detail for detectors incorporating angular-biased MCPs. It was found that the presence of the pore bias at the output MCP results in a variation of the charge footprint position for events with different gains. Events with higher gains are shifted in the direction of the pore bias and the absolute value of this shift is directly proportional to the absolute value of the detector gain. Variation of the detector modal gain from 7.5×10^6 to 2.5×10^7 resulted in a $\sim 100 \mu\text{m}$ image offset for a 13° -biased MCP positioned at a distance of 8.5 mm from the anode with an accelerating rear field of 75 V/mm. We also extended our previous study of another type of detector walk associated with fluctuations of the accelerating rear field. Image displacements as functions of the rear accelerating field for both 13° - and 19° -biased MCPs were measured and compared with the results of computer simulation based on our charge cloud propagation model presented earlier. A good agreement between the experimental and simulated data verifies the validity of the model for different MCPs. © 2000 American Institute of Physics. [S0034-6748(00)00311-7]

I. INTRODUCTION

Recent advances in readout techniques and processing electronics have resulted in a substantial improvement of the spatial resolution of imaging detectors based on microchannel plates (MCPs). For instance, a position resolution of $\sim 15 \mu\text{m}$ full width at half maximum (FWHM) was demonstrated with delay-line anodes,¹ and less than $10 \mu\text{m}$ FWHM with both a Vernier readout^{2,3} and subpixel centroiding in an intensified charge-coupled device.⁴ As a result, it is now believed that the overall imaging performance of these detectors is limited by the microchannel plate pore spacing³⁻⁵ (8–15 μm in conventional MCPs). The ongoing developments in the production process of glass MCPs should provide the commercial availability of small pore ($<6 \mu\text{m}$) channel plates.⁶ However, it was reported that reduction of the MCP pore size actually eliminates the fixed pattern noise in the flat field images.⁷ Even much smaller (submicron) pore sizes should become available with the emerging manufacturing techniques, which should enable the production of silicon-micromachined⁸ and anodic aluminum oxide MCPs.^{9,10} The spatial resolution of such detectors will again be limited by the accuracy of the readout element and signal processing electronics. However, we observed experimentally that in high-accuracy imaging MCP detectors yet another important phenomenon should be taken into account, namely, the image blurring along the pore bias axis, characteristic to detectors with a biased (usually 5° – 13°) output microchannel plate. In this article, we present the study of two different mechanisms leading to these image displace-

ments. These mechanisms are associated with the two different factors influencing the event centroid position, namely, the absolute event gain and the accelerating field between the MCPs and the anode.

We have already discussed the effect of the ballistic offset of event centroids caused by the presence of an angular microchannel bias at the rear MCP.¹¹ It was observed experimentally and simulated that the charge cloud leaving the rear MCP has a finite transverse velocity in the direction of the channel bias. Depending on the time of the cloud propagation to the anode, the position of the cloud centroid will be offset in this direction. With a fixed detector gain, accelerating rear field, and distance between the MCPs and the readout element, this offset is constant for the entire active area and does not contribute to any image distortions. However, we showed that the fluctuations of the accelerating rear field (characteristic to some detectors with the rear field controlled by voltage dividers, for example) can lead to degradation of spatial resolution along the pore bias. The image offset (which we will refer to as detector walk) was studied previously as a function of accelerating field.¹¹ Along with that, we found that the charge footprint centroid also depends on the MCP stack gain for each individual event.^{12,13} Since each MCP stack location features a certain gain range, commonly characterized as a pulse height distribution function of a detector, the image offset always varies along the axis of the pore bias, which in some cases may degrade the detector spatial resolution. In Sec. II, we present our detailed study of the image offset as a function of the detector gain (detector walk with gain). We also extended our previous study of the image offset as a function of the rear accelerating field and distance¹¹ in Sec. III. In addition to 13° -biased MCP data,

^{a)}Electronic mail: ast@ssl.berkeley.edu

image displacements were measured and modeled for newly available MCPs with pores tilted by 19° relative to the MCP normal.

II. DETECTOR WALK WITH GAIN

The statistical variation of the MCP stack gain is generally characterized by the pulse height distribution with typical values of FWHM of about 20%–50%. Many readout techniques encoding the position of the charge cloud centroid are tolerant to this gain variation, i.e., within this range of relative gain variations the spatial resolution of the readout anode and signal processing electronics is virtually independent of the event gain. However, we observed that the actual position of the charge cloud centroid changes with gain for detectors with an angular-biased output MCP, commonly used to prevent ion feedback. Apparently, the charge cloud centroid position changes along the axis of the channel pore bias. We call this effect detector walk by analogy with electronic walk where the output signal is a function of gain. The presence of these image shifts may degrade the overall spatial resolution of some high-accuracy detectors, where the resolution is believed to be limited by the channel pore diameter.^{3–5} The promising ongoing developments in the new MCP production technologies should result in a substantial reduction of the pore sizes, and therefore, detector walk described here may become an essential factor limiting the resolution of future instruments.

We studied the detector walk phenomenon with a detector consisting of a Z-stack of microchannel plates and a cross-delay-line readout anode,¹² which provided good linearity and resolution of about $25\ \mu\text{m}$ FWHM. The microchannel plate stack consisted of three 80:1 L/D, $12.5\ \mu\text{m}$ pores on $15\ \mu\text{m}$ centers, 36 mm in diameter MCPs from Photonis-SAS with resistances of $\sim 30\ \text{M}\Omega$, channel end spoiling of 1 pore diameter and a pore bias of 13° . The MCP voltage varied between 3300 and 3800 V, corresponding to the detector modal gain variation between 8×10^6 and 2.5×10^7 . A typical pulse height FWHM was about 25%. An accelerating bias of 75 V/mm was applied from a separate voltage source in the 8.5 mm gap between the MCPs and the readout anode. A pinhole mask was installed directly on the front surface of the MCP stack ($10\ \mu\text{m}$ pinholes on a 0.5-mm-spaced grid). A mercury vapor pen-ray lamp (2537 Å) was used for the illumination, and a number of pinhole mask images were accumulated at a count rate of $\sim 1.5\ \text{counts}\cdot\text{s}^{-1}$ per pinhole. Each image contained about 3×10^5 events with ~ 1000 pinholes in the entire image.

First, the MCP pore bias was aligned along the X axis of the detector. The pinhole mask images were then recorded at several MCP voltages varying between 3300 and 3700 V. The image files contained the lists of corresponding gain and coordinates for each registered photon. Consequently, the position of each pinhole as a function of gain could be extracted from that data. We represent these data in the form of walk plot images, where the intensity of each pixel corresponds to the number of registered photons for particular gain and coordinate (x or y). Figure 1 shows the plot of a combined x -axis walk extracted from three photon lists taken

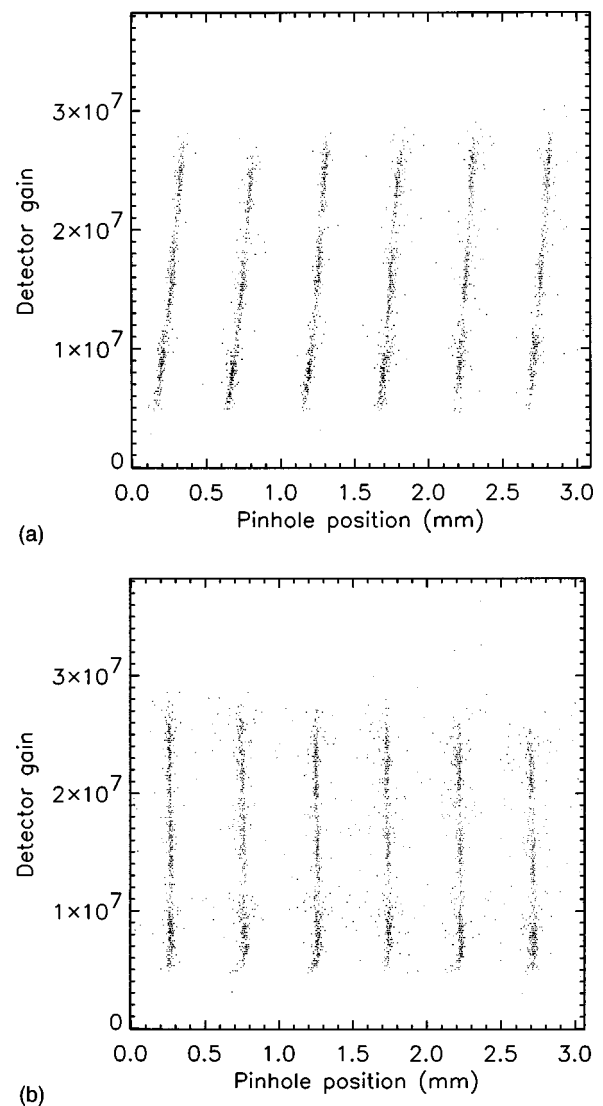


FIG. 1. x -axis (a) and y -axis (b) detector walk plots extracted from the data obtained with 13° -biased MCPs with a pore bias directed along the x axis, 8.5 mm gap between the MCPs and the readout anode. The position of each photon from six pinholes is plotted as a function of the event gain. Pinhole mask images were recorded in the form of photon lists at three detector modal gains of 8×10^6 , 1.6×10^7 , and 2.1×10^7 (three corresponding separate stripes, one for each pinhole data). The displacement of the registered photon along the direction of the pore bias is apparent for events with higher gains. There are no displacements along the y axis.

at 3300, 3500, and 3700 V MCP voltages (corresponding detector modal gains of 8×10^6 , 1.6×10^7 , and 2.1×10^7). As seen in Fig. 1, the data for each pinhole consist of three “stripes” corresponding to the three MCP voltages. The x position of the photon is apparently in direct proportion to the event gain, Fig. 1(a), with larger values of the x coordinate corresponding to larger gain. In other words, the displacement of the registered photon from its original position along the direction of the pore bias (x axis) increases with event gain. The fact that the three stripes on the plot of each pinhole walk lie along straight lines, indicates that the event position is solely a function of the absolute detector gain and it is independent of the MCP voltage. The y -axis walk plot extracted from the same data set is shown in Fig. 1(b). There is no dependence of the encoded photon y position on the detector gain.

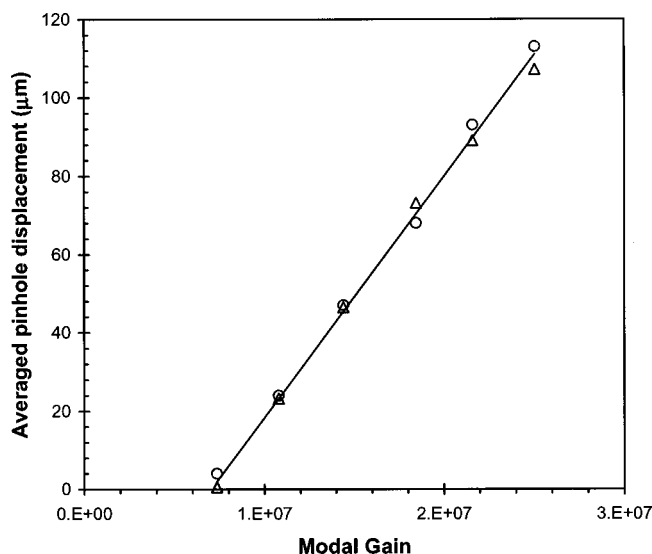


FIG. 2. Relative image displacement as a function of the detector modal gain for 13° -biased MCPs positioned at a distance of 8.5 mm to the readout anode. The displacement is averaged over 1000 pinholes from each image. Triangles represent the data obtained with the pore bias aligned along the x axis, while no displacements were observed along the y axis. Circles correspond to the data obtained with the MCP stack rotated by 90° (image displacements along the y axis in that case).

The relative displacements of the centroid of each pinhole footprint from one image to another were then extracted from the data measured at different MCP voltages. The value of that displacement along the pore bias, averaged over ~ 1000 pinholes, is shown in Fig. 2, where the two types of markers correspond to the two orthogonal orientations of the MCP stack. One can see that within the measured range of modal gains the encoded pinhole position along the pore bias is directly proportional to the detector gain.

The values of the image displacement in Fig. 2 indicate that the spatial resolution of high-accuracy imaging detectors incorporating angular-biased MCPs at the last stage of electron multiplication may be impaired along one axis by the presence of such detector walk with gain. The entire image may thus be blurred along the axis of the channel pore bias if the spatial resolution of the detector is high enough (on the order of $10 \mu\text{m}$). In our opinion, the detector walk can be explained by the different momentum and energy distributions of the output charge cloud depending on the gain and saturation of each event. Although the exact explanation of the walk phenomena is not known to us, we assume that events with higher gain correspond to a higher level of MCP pore saturation and, consequently, more collimated charge cloud distribution at the pore output, resulting in a larger offset of the event centroid.

In order to verify that the observed event displacements were not an artifact induced by the readout anode or processing electronics, the microchannel plate stack was rotated by 90° within the detector. The same measurements were then repeated and we observed that the detector walk followed the direction of the rear MCP pore bias, so that x - and y -axes walk plots merely swapped.

We then replaced the MCP stack with a set of three microchannel plates, which had a zero-degree-biased output

MCP (with front and middle plates still 13° biased) and repeated the same measurements as with the previous MCP stack in Z configuration. No detector walk with gain was observed in that experiment. Both x - and y -axes walk plots (not shown) were similar to the plot presented in Fig. 1(b). The encoded photon position did not depend on the detector gain. By rotating the MCP stack and replacing the rear MCP by a zero-biased one, it was proved that this detector walk is determined solely by the presence of inclination of the output MCP pores and that the direction of this walk is along the axis of the pore bias.

We conclude from the results of our study that optimization of the detector parameters such as the FWHM of its pulse height distribution, rear accelerating field, and distance, is necessary if detector walk with gain is on the order of the detector spatial resolution. An alternative is to utilize a zero-degree-biased MCP as the output plate in the stack, although a further study of the ion feedback phenomena is necessary in that case.

III. IMAGE DISPLACEMENT AS A FUNCTION OF REAR FIELD

A detailed study of the image displacement as a function of the rear accelerating field (the electric field between the MCPs and the readout element) was presented earlier for 13° -biased microchannel plates.¹¹ We showed that fluctuations of the rear accelerating field (for example, due to MCP resistance fluctuations in devices with voltage dividers) result in translational shifts of the entire image, thus degrading the detector spatial resolution. The results of our computer simulation of the image displacements for 13° -biased MCPs proved to be in a very good agreement with the experimental data. In our calculations of image displacements we used the experimentally measured charge cloud distribution function $f(E, \theta)$ at the MCP output¹⁴ (E and θ are the output energy and angle, correspondingly). Provided the energy and angle are known from $f(E, \theta)$ for each output electron and the position of each electron at the anode is calculated from a ballistic trajectory, the charge distribution function $\rho(r, \varphi)$ at the plane of the anode can be calculated from the distribution function $f(E, \theta)$. The event centroid can be easily obtained then from the function $\rho(r, \varphi)$. A detailed description of the model can be found in our previous publications.^{11,13}

In this study, the validity of computer simulation of the MCP electron cloud propagation (and, consequently, the detector walk with rear accelerating field) was further verified with newly available 19° -biased MCPs, where the image shifts are more pronounced than in our previous report. The comparison of experimentally measured and simulated data should be more accurate in that detector configuration, since the image displacement for 19° -biased MCPs is more pronounced, although it depends also on the distance d between the MCP stack and the readout element.

A set of three microchannel plates in Z configuration was used in the present measurements. MCPs procured from Photonis were 75 mm in diameter and had a pore size of $10 \mu\text{m}$ on $12 \mu\text{m}$ centers, 19° bias angle, 80:1 L/D, and resistance of $\sim 30 \text{ M}\Omega$. Photon event positions were read out with

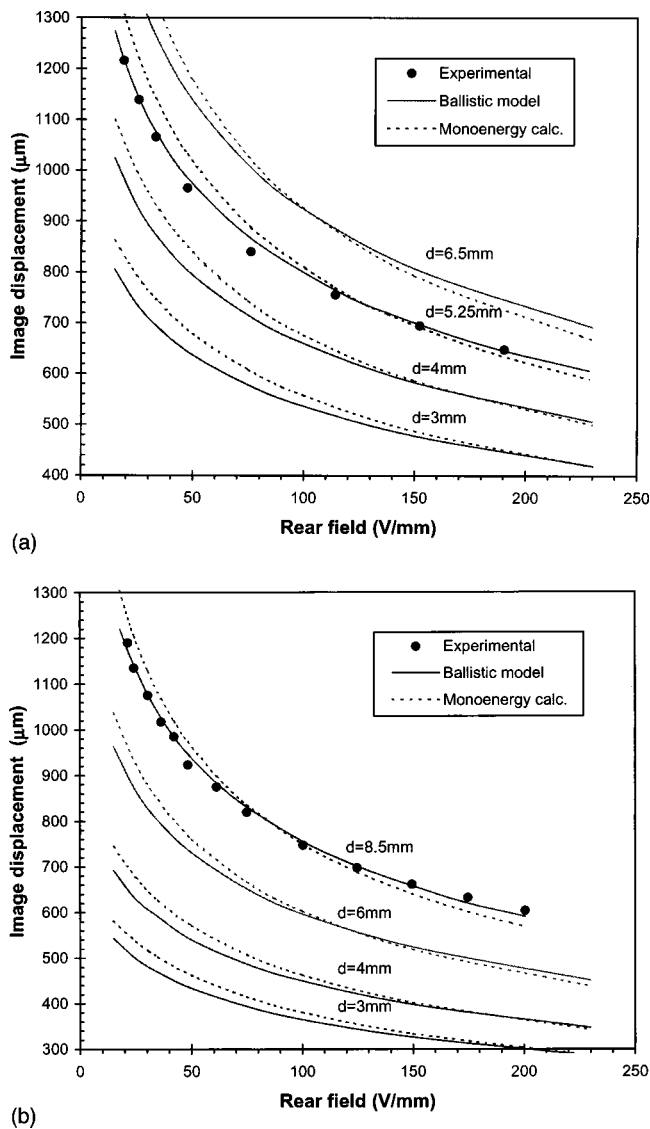


FIG. 3. Measured and calculated image displacement as a function of the accelerating rear field. (a) 19° MCP pore bias. (b) 13° MCP pore bias. Circles correspond to the experimentally measured data, adjusted by a constant for comparison with the calculation results (only relative values of the shifts were measured). Solid curves, the results of our calculations with the ballistic model of the charge cloud propagation (see Refs. 11 and 13). Dashed curves, monoenergy calculations (see Ref. 11).

a cross-delay-line anode and associated electronics, designed for the GALEX mission.¹⁵ A pinhole mask with $10\ \mu\text{m}$ holes on a 1-mm-spaced grid was installed directly on the front surface of the MCP stack. The spatial resolution of the detector was $\sim 30\ \mu\text{m}$ FWHM. The MCP stack gain was about 2×10^7 and an independently controlled accelerating bias of 100–1000 V was applied in the 5.25 mm gap between MCPs and the readout anode. A number of pinhole mask images was recorded at count rates of $\sim 1.2\ \text{counts}\cdot\text{s}^{-1}$ per pinhole and each image contained about 3×10^5 events with 320 pinholes in the entire image. The relative displacement of the centroid of each pinhole footprint from one image to another

was extracted from that data set. The averaged displacement is presented in Fig. 3(a) as a function of the accelerating field. Circles correspond to the experimentally measured data, while the curves are the results of our calculations with the ballistic model of the charge cloud propagation,^{11,13} which takes into account the charge angular and energy distributions (solid curves), and the monoenergy calculations¹¹ (dashed curves). Figure 3(b) shows the same data for 13° -biased MCPs (the measurement details are described in Ref. 11). The measurements of image displacement provided only the relative shifts between the different images, rather than their absolute values. Therefore, the same constant is added to all experimental data for comparison with the results of our calculations, which provide the absolute values of the shift.

A good agreement between the results of computer simulation and the experimentally measured image displacements for both 13° - and 19° -biased MCPs verifies the validity of the ballistic model of the charge cloud propagation. The parameters of the charge distribution function we used in the model (measured by Bronshtein *et al.*¹⁴) appear to be valid for a conventional MCP with the end spoiling of one channel diameter. The model, therefore, can be used for extending our data to different detector parameters and configurations. Thus, computer simulation can substantially reduce the time necessary for optimization of detector resolution in future experiments.

ACKNOWLEDGMENT

This study was supported by NASA Grant No. NAG5-3913.

- ¹O. H. W. Siegmund *et al.*, Proc. SPIE **3114**, 283 (1997).
- ²J. S. Lapington, B. S. Sanderson, and L. B. Worth, Proc. SPIE **3445**, 535 (1998).
- ³J. S. Lapington, B. Sanderson, and L. B. C. Worth, Proceedings of the 5th International Conference on Position-Sensitive Detectors, University College London, 13–17 September (1999) (to be published).
- ⁴J. V. Vallergera, O. H. W. Siegmund, J. Dalcomo, and P. N. Jelinsky, Proc. SPIE **3019**, 156 (1997).
- ⁵J. S. Vickers and S. Chakrabarti, Rev. Sci. Instrum. **70**, 2912 (1999).
- ⁶B. N. Laprade, R. C. Cochran, F. Langevin, and M. W. Dykstra, Proc. SPIE **3173**, 474 (1997).
- ⁷O. H. W. Siegmund, M. A. Gummin, T. Ravinett, S. R. Jelinsky, and M. L. Edgar, Proc. SPIE **2808**, 98 (1996).
- ⁸C. P. Beetz, R. B. Boerstler, J. Steinbeck, B. Lemieux, and D. R. Winn, Nucl. Instrum. Methods Phys. Res. A **442**, 443 (2000).
- ⁹R. C. Furneaux, W. R. Rigby, and A. P. Davidson, Nature (London) **337**, 147 (1989).
- ¹⁰A. Govyadinov, I. Emeliantchik, and A. Kurilin, Nucl. Instrum. Methods Phys. Res. A **419**, 667 (1998).
- ¹¹A. S. Tremsin, J. V. Vallergera, and O. H. W. Siegmund, Proceedings of the 5th International Conference on Position-Sensitive Detectors, University College London, 13–17 September (1999) (to be published).
- ¹²J. V. Vallergera and O. H. W. Siegmund, Nucl. Instrum. Methods Phys. Res. A **442**, 159 (2000).
- ¹³A. S. Tremsin and O. H. W. Siegmund, Rev. Sci. Instrum. **70**, 3282 (1999).
- ¹⁴I. M. Bronshtein, A. V. Yevdokimov, V. M. Stozharov, and A. M. Tyutikov, Radio Eng. Electron. Phys. **24**, 150 (1979).
- ¹⁵O. H. W. Siegmund *et al.*, Proc. SPIE **3765**, 429 (1999).